

Spin-Polarization Mechanisms of the Nitrogen-Vacancy Center in Diamond

Delaney, P., Greer, J. C., & Larsson, J. A. (2010). Spin-Polarization Mechanisms of the Nitrogen-Vacancy Center in Diamond. *Nano Letters*, 10(2), 610-614. DOI: 10.1021/nl903646p

Published in:
Nano Letters

Queen's University Belfast - Research Portal:
[Link to publication record in Queen's University Belfast Research Portal](#)

General rights

Copyright for the publications made accessible via the Queen's University Belfast Research Portal is retained by the author(s) and / or other copyright owners and it is a condition of accessing these publications that users recognise and abide by the legal requirements associated with these rights.

Take down policy

The Research Portal is Queen's institutional repository that provides access to Queen's research output. Every effort has been made to ensure that content in the Research Portal does not infringe any person's rights, or applicable UK laws. If you discover content in the Research Portal that you believe breaches copyright or violates any law, please contact openaccess@qub.ac.uk.

Spin-Polarization Mechanisms of the Nitrogen-Vacancy Center in Diamond

Paul Delaney,^{*,†} James C. Greer,[‡] and J. Andreas Larsson[‡]

[†]Queen's University Belfast, University Road, Belfast, BT7 1NN, Northern Ireland, and [‡]Tyndall National Institute, University College Cork, Lee Maltings, Prospect Row, Cork, Ireland

ABSTRACT The nitrogen-vacancy (NV) center in diamond has shown great promise for quantum information due to the ease of initializing the qubit and of reading out its state. Here we show the leading mechanism for these effects gives results opposite from experiment; instead both must rely on new physics. Furthermore, NV centers fabricated in nanometer-sized diamond clusters are stable, motivating a bottom-up qubit approach, with the possibility of quite different optical properties to bulk.

KEYWORDS Nitrogen-vacancy (NV) center, diamond, qubit, spin polarization

The nitrogen-vacancy (NV) center in diamond is a rich testbed for quantum information: it is a promising source of single photons^{1,2} and can implement the two-qubit controlled-rotation gate (CROT).³ Two properties are key to its success: the triplet electronic ground state can be *spin-polarized* to S_z by optical radiation to initialize the qubit,⁴ while the *higher fluorescence* from S_z reads out the qubit state optically.⁵ The leading mechanism for these properties has been intersystem crossing to the 1A_1 or 1E singlets, and recently this was shown to indeed produce S_z spin polarization if 1A_1 is the lowest singlet;^{6,7} however previous calculations disagreed on their energies and ordering.^{8,9} Here we show that 1E lies below 1A_1 using fully correlated configuration interaction calculations. With our current understanding, intersystem crossing would then cause S_x and S_y spin polarization, contrary to what is observed. Thus NV qubit initialization and readout must use presently unknown physics. If something so fundamental to the operation of the NV center is yet to be unraveled, there must be much left to be found and explored in this already very useful defect.

Following Manson et al.,^{6,7} Figure 1 shows the schematic electronic structure of the unstrained NV⁻ center. The ground term is a spin-triplet of symmetry 3A_2 in C_{3v} (irreps a_1, a_2, e) split by the spin–spin interaction into an A_1 symmetry $|A_2, S_z\rangle$ level 2.88 GHz below a degenerate E pair $|A_2, S_y\rangle, |A_2, S_x\rangle$.^{6,10} Here $\hat{S}_x S_x = \hat{S}_y S_y = \hat{S}_z S_z = 0$; S_z has A_2 symmetry while the pair S_x, S_y transform as E. There is a strong optical transition to an excited triplet term 3E with a zero-phonon line (ZPL) of 1.945 eV (637 nm).¹¹ The axial spin–orbit interaction splits 3E into three pairs of symmetry E, E', and (A_1, A_2): this last pair is then split by the spin–spin interaction.^{6,7}

The ground term can be spin-polarized to its $A_1 |A_2, S_z\rangle$ level by optical excitation at 532 nm (2.33 eV) to the vibronic

sideband of the excited triplet 3E .⁴ We can use the larger photoluminescence intensity from the $A_1 |A_2, S_z\rangle$ level than from the E pair $|A_2, S_y\rangle, |A_2, S_x\rangle$ to read-out the qubit.⁵ The spin state is unchanged by electric dipole transitions, hence the focus on intersystem crossing (ISC) to the metastable 1A_1

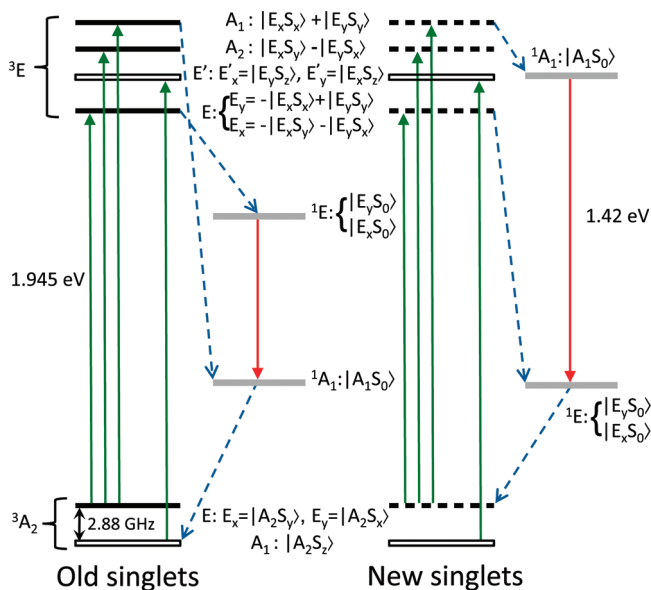


FIGURE 1. Electronic structure of the unstrained NV⁻ center. The 3A_2 and 3E terms (experimental ZPL 1.945 eV) have spin–spin and spin–orbit splittings greatly exaggerated for clarity. States are labeled by symmetry and approximate wave functions from ref 6: S_x, S_y polarization is solid, S_z is hollow, S_0 is gray. Vertical upward arrows (green) show net transitions following 532 nm (2.33 eV) electric dipole excitation and spin-preserving relaxation. (Left) The singlet structure widely assumed correct to date: 1A_1 lowest. Dashed arrows (blue) show allowed intersystem decay paths (assuming a_1 phonons participate) which feed into the ground A_1 level giving S_z spin-polarization. (Right) Singlet order predicted by this work: 1E is lowest with 1A_1 close to 3E (the $^1A_1, ^3E$ order is unknown). The $^1E \leftrightarrow ^1A_1$ vertical excitation difference is calculated to be 1.42 eV (see text); electric dipole (red downward arrows) and/or nonradiative transitions cause fast decay from 1A_1 . The same assumptions now give S_x, S_y spin-polarization, contradicting experiment.

* Corresponding author, p.delaney@qub.ac.uk.

Received for review: 10/31/2009

Published on Web: 01/19/2010

TABLE 1. Vertical Excitation Energies ΔE_v of the NV⁻ Center.^a

symmetry	short wave function	DFT/von Barth	Goss ⁸ DFT	Gali ⁹ DFT	C ₂₈₄ H ₁₄₄ N ⁻ DFT	C ₄₂ H ₄₂ N ⁻ DFT	C ₄₂ H ₄₂ N ⁻ CI	N _{CSF} CI
³ E	$\begin{cases} E_y \\ E_x \end{cases}$	$ vx\bar{x}y\rangle$	1.77	1.910	1.898	1.270	1.958	68669
		$ vxy\bar{y}\rangle$						
¹ A ₁		$(1/2^{1/2})[v\bar{v}x\bar{x}\rangle + v\bar{v}y\bar{y}\rangle]$	1.67	≈0.0	2.028	2.096	2.060	83721
¹ A'		$ v\bar{v}x\bar{x}\rangle$			1.255	1.259		
¹ E	$\begin{cases} E_y \\ E_x \end{cases}$	$(1/2^{1/2})[v\bar{v}x\bar{y}\rangle - v\bar{v}x\bar{y}\rangle]$	0.44	≈0.9	0.482	0.422	0.629	88274
		$(1/2^{1/2})[v\bar{v}y\bar{y}\rangle - v\bar{v}x\bar{x}\rangle]$						
A''		$ v\bar{v}x\bar{y}\rangle$			0.241	0.211		
³ A ₂		$ v\bar{v}x\bar{y}\rangle$	0	0	0	0	0	83434

^a Energies are in eV and measured from the ³A₂ ground state. For wave functions we take the case $m_s = S$, orbitals u and below are completely filled and suppressed, bars denote down spin and C_{3v} matrices are as in ref 13. DFT energies for multireference states use von Barth's method;¹⁸ the last column gives N_{CSF}.

and ¹E levels arising from the ³A₂ configuration to explain both effects.

The best mechanism so far proposed is by Manson et al.,^{6,7} see Figure 1 (left). An NV center initially in the $E_x = |A_2, S_y\rangle$ or $E_y = |A_2, S_x\rangle$ levels of the ground state absorbs 532 nm radiation and then decays to the A₁, A₂ or E levels of the ³E term, assuming spin-projection is preserved. *If the ¹E level is neglected*, an ISC to the ¹A₁ level can occur only from the A₁ level, if the energy is carried away by symmetric (a_1) phonons, as the Hamiltonian terms generating transitions have A₁ symmetry. A second similar ISC to the ground term can then only relax to its A₁ level, which has S_z polarization. On the other hand, a center initially in the A₁ symmetry $|A_2, S_z\rangle$ level can be excited to E' but is then forbidden by symmetry from ISC to the ¹A₁ level: S_z spin-polarization of the center results. *If a ¹E level between ¹A₁ and ³E is included*, the decreased energy gaps and new pathway (³E)E → ¹E → ¹A₁ → (³A₂)A₁ increases the S_z polarization (E' → ¹E is forbidden),⁶ but *if the ¹E level lies below ¹A₁* the explanation fails, as ¹E would relax to the E_x, E_y ground levels with spin polarization S_y, S_x (Figure 1, right). Unlike the triplets for which decent density functional theory (DFT) calculations exist,^{8,9,12,13} the singlets are of *multireference* character and calculations differ greatly in their energies and ordering.^{8,9} Despite the unreliability of calculations, it has been widely assumed that ¹A₁ < ¹E with ¹E commonly being neglected leading to figures with just the ¹A₁ level between the triplets which are ubiquitous in the literature. Using configuration interaction (CI) calculations we shall show the ¹E level lies below the ¹A₁, prompting the search for a new explanation of NV⁻ spin-polarization.

The atomic origins of these many-body levels are described in several papers.^{8,9,12-14} Dangling sp³ bonds a, b, c on the three carbon atoms and d on the nitrogen atom pointing toward the vacancy mix to form four molecular orbitals u, v, x, y with energy ordering $u < v < x = y$. Both u and v are of symmetry a_1 while x, y transform as e . For the negatively charged defect NV⁻, we fill these orbitals with six electrons. The *vacancy model* assumes that occupying just these states in different ways gives the low-energy electronic structure.¹⁵

Columns 1 and 2 of Table 1 give symmetries and high- m_s model wave functions belonging to the $u^2v^2e^2$ and $u^2v^1e^3$

configurations. Focusing on the ³A₂ ground term and the ³E term of the excited configuration separated by the 1.945 eV ZPL, we see the $m_s = 1$ components of both levels can be modeled using single Slater determinants. DFT—a ground state theory—can calculate properties of the lowest many-body state in each spatial and spin symmetry,¹⁶ although the exchange-correlation functional $E_{xc}[\rho]$ should then be symmetry-dependent. Neglecting this as is traditional for single-reference states such as ³E leads to DFT estimations of the vertical excitation energies ΔE_v (here always with respect to the ³A₂ ground state) in column 3 by Goss et al. using the vacancy-centered cluster C₃₃H₃₆N⁻,⁸ in column 4 by Gali et al. using a 512-atom simple cubic supercell⁹ and in column 5 this work's values for C₂₈₄H₁₄₄N⁻¹³ in C_s symmetry (see below). DFT only appears to get excellent agreement with the ZPL: there is a fortuitous cancellation between DFT underestimation and neglected relaxation.¹⁷

Also belonging to the $u^2v^2e^2$ configuration of the ground state are the metastable singlets of symmetry ¹E and ¹A₁. From column 2 their multireference nature can be seen;¹³ in such cases von Barth showed that neglect of the symmetry dependence of $E_{xc}[\rho]$ can cause severe errors.¹⁸ His proposal was to take linear combinations of pure-symmetry multireference states to form single determinants of mixed symmetry and then use electron-gas $E_{xc}[\rho]$ only for these single-determinant energies E; these are usually accurate as the pair-correlation function is well-described. These wave functions are not eigenstates—E is an expectation value and a linear combination of the energies of the constituent pure-symmetry states—but if sufficient mixed determinants are formed from a given configuration, we can solve these linear equations for the pure-symmetry energies we desire.

Applying this to the NV center, DFT can calculate total energies E of the excited determinants $|v\bar{v}x\bar{x}\rangle$ and $|v\bar{v}x\bar{y}\rangle$ which are constituents of the ¹E and ¹A₁ levels (Table 1, column 2) if we lower the wave function symmetry to C_s (irreps a', a'') to allow independent occupation of x and y , while keeping the geometry of the C_{3v} relaxation. The true ΔE_v are then estimated from the formulas

$$\Delta E_v(^1A_1) = 2[E(|v\bar{x}\bar{x}\rangle) - E(|v\bar{x}y\rangle)]$$

$$\Delta E_v(^1E) = 2[E(|v\bar{x}y\rangle) - E(|v\bar{y}x\rangle)]$$

where $E(|v\bar{x}y\rangle)$ is the ground state energy. However, while column 3 shows Goss's energy ordering to be $^3A_2 < ^1E < ^1A_1$ with energies 0.00, 0.44, and 1.67 eV,⁸ column 4 shows Gali's findings: the singlets are in the opposite order, $^3A_2 < ^1A_1 < ^1E$, with energies 0.0, ≈ 0.0 , ≈ 0.9 eV.⁹ Column 5 shows our DFT predictions for the $C_{284}H_{144}N^-$ cluster which agree with the energy order of Goss. If $^1E < ^1A_1$ is the true order, a new explanation for spin polarization must be sought; however given the disagreements and neglect of the symmetry dependence of $E_{xc}[\rho]$, DFT energies cannot be taken as definitive.

Such multireference states are described more naturally within configuration interaction. In CI the many-body wave function Ψ is expanded in a subset of the complete set of all Slater determinants Ψ_i formed from $2m$ molecular spin orbitals by filling them with n electrons. To reduce the number of coefficients c_i we expand in configuration state functions (CSFs) $\tilde{\Psi}_i$: Slater determinants projected onto a given S^2 value

$$\Psi = c_1 \tilde{\Psi}_1 + c_2 \tilde{\Psi}_2 + \dots + c_{N_{\text{CSF}}} \tilde{\Psi}_{N_{\text{CSF}}}$$

The $2m$ spin orbitals typically come from a DFT or Hartree–Fock calculation. Solving $H\Psi = E\Psi$ in this space is a straightforward but large eigenvalue problem. Analytic formulas for the matrix elements are known when the molecular orbitals are built from Gaussians.

The difficulty with CI is the combinatorial explosion of the number of possible Slater determinants $N_{\text{SD}} = \binom{2m}{n}$: CI scales badly with system size. No wave-function-based method can handle the $C_{163}H_{100}N^-$ and $C_{284}H_{144}N^-$ clusters of our recent work;¹³ hence we use the smaller cluster $C_{42}H_{42}N^-$ (Figure 2). For it and $C_{284}H_{144}N^-$, we compute the optimized DFT ground-state geometries in C_{3v} using the Becke–Perdew exchange–correlation functional and DZV(P) basis set from the TURBOMOLE suite of programs.¹⁹ For $C_{42}H_{42}N^-$ we then reduce the number of active electrons by using effective core potentials (ECPs) and the double- ζ (DZ) basis set on all carbons except the central three, where together with the nitrogen the DZV(P) basis set is used. Hydrogens are treated with a DZ basis set.

Before CI results are accepted, we must first show that $C_{42}H_{42}N^-$ with reduced basis set and ECPs is still a good model of the NV center in bulk diamond, as the center might either cease to exist or be greatly altered in such small clusters. Column 6 of Table 1 shows our DFT results for

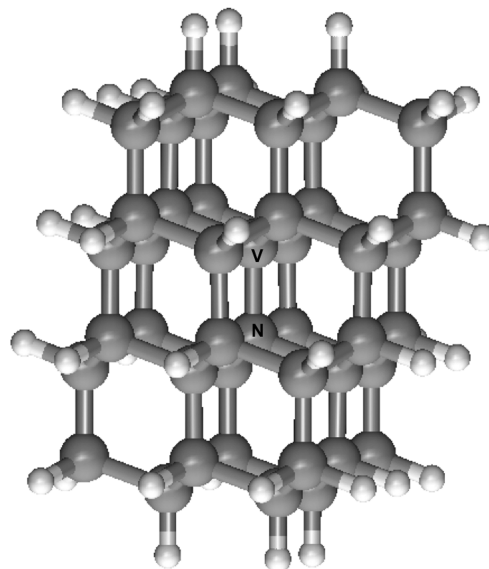


FIGURE 2. The $C_{44}H_{42}$ diamond cluster. $C_{42}H_{42}N^-$ is built from it by removing the carbon atom marked V and replacing its neighbor marked N with a nitrogen atom.

$C_{42}H_{42}N^-$. The location of the singlets is remarkably unchanged; the main effect of the smaller cluster is a substantial lowering of the 3E term by ≈ 0.6 eV within DFT. Examining DFT molecular orbital energies, we see a related decrease in the $v \leftrightarrow e$ gap, which shrinks by 0.4 eV for spin-up and 0.6 eV for spin-down.²⁰ To quantify the effect of the reduced basis set and ECPs, we performed all-electron calculations using the DZV(P) basis set and found negligible change in $\Delta E_v(^3E)$: the differences are due to the reduced cluster size. For the smaller cluster $C_{33}H_{36}N^-$, Goss also finds a lower-than-average $\Delta E_v(^3E)$,⁸ though the smaller reduction suggests that the 3E energy is quite dependent on cluster geometry. Although the $v \leftrightarrow e$ gap decreases, this tends to cancel in energy differences between the 3A_2 , 1E , 1A_1 terms as they all arise from the configuration $u^2v^2e^2$, explaining the stability of their ΔE_v . Table 2 shows that DFT bond distances and angles are adequately described in $C_{42}H_{42}N^-$: the single change is a 0.145 Å increase in the distance N– C_V between the nitrogen and the three central carbons, possibly related to the decrease in the ZPL. Summarizing, the NV center persists in $C_{42}H_{42}N^-$; singlet energies $\Delta E_v(^1E)$ and $\Delta E_v(^1A_1)$ are unchanged from bulk diamond, while the ZPL reduces with size.

The quality of the CI calculation also depends on the number, N_{CSF} , of configuration state functions used in the expansion. We employ the Monte Carlo CI technique of Greer,²¹ keeping CSFs whose coefficients obey $|c_i| > c_{\text{min}}$ with $c_{\text{min}} = 0.00025$, which provides accurate results for ΔE_v .²² Convergence in c_{min} was tested by running with the less accurate value $c_{\text{min}} = 0.0005$, giving $N_{\text{CSF}} \approx 13000$: on doing so the three vertical excitation energies $\Delta E_v(^1E)$, $\Delta E_v(^1A_1)$, and $\Delta E_v(^3E)$ systematically decreased by the small amounts 0.034, 0.065, and 0.051 eV, respectively, giving us confidence in the predicted energy ordering. Column 7 of Table

TABLE 2. Cluster Geometry^a

cluster	N–C _N	N–C _V	C _V –C			∠C ₃ –N–C _N
C ₄₂ H ₄₂ N [−]	1.481	2.916	1.500	1.503	1.503	105.5
C ₂₈₄ H ₁₄₄ N ^{−13}	1.478	2.771	1.511	1.511	1.513	105.1

^a Distances in angstroms and angles in degrees. C_N are the three carbon neighbors of the nitrogen, C_V are the three carbon neighbors of the vacancy. ∠C₃–N–C_N is the angle between the C₃ symmetry axis and an N–C_N bond.

1 has the CI ΔE_V for $c_{\min} = 0.00025$: the last column (8) gives N_{CSF} . The CI results show clearly that the ¹E singlet lies below the ¹A₁: the small ≈ 0.02 eV splitting in the ¹E energies is due to different Monte Carlo sampling for the E_x and E_y wave functions and gives another estimate of our CI error. The ¹E ↔ ¹A₁ gap of 1.42 eV (downward vertical line in Figure 1 (right)) is in fair agreement with the 1.19 eV (1046 nm) ZPL recently observed by Rogers et al.⁷ and attributed to a ¹E ↔ ¹A₁ transition, the difference probably being due to relaxation. However, relaxation is very unlikely to change the order of the singlets, leaving us with the clear conclusion that the ¹E is the lowest singlet and that spin polarization, key to the NV center's attractiveness, is caused by unknown physics.

That this ordering makes the most sense is shown by its consistency with DFT in three out of four calculations: our C₄₂H₄₂N[−] and C₂₈₄H₁₄₄N[−] clusters and the C₃₃H₃₆N[−] cluster calculation of Goss,⁸ Gali's results are the only exception. Among these three calculations the agreement is also quantitative: DFT underestimates the ¹E energy by ≈ 0.15 – 0.2 eV while our DFT ¹A₁ level is ≈ 0.04 eV too high and that of Goss is ≈ 0.4 eV too low. If Gali's result can be ignored, it seems that von Barth's method is quite good for the NV singlets. This ordering is also consistent with the results of Zyubin et al. for the considerably smaller clusters C₃NVH₁₂ and C₁₉NVH₂₈.²³

The ¹A₁ and ³E levels are close for C₂₈₄H₁₄₄N[−] in DFT and C₄₂H₄₂N[−], meaning that fewer phonons are needed for ISC giving fast transitions. Experimental work has also supported closeness of ¹A₁ and ³E: using a three-level model of the temperature-dependence of delayed fluorescence Dräbenstedt et al. predicted that ¹A₁ lies < 37 meV below ³E.²⁴ This closeness also makes it unlikely that computation can determine the ¹A₁, ³E ordering. This is particularly so in large systems where only DFT is feasible, as there are two significant errors in ΔE_V (³E): a DFT underestimation of ≈ 0.3 eV nearly canceling with the neglect of relaxation of order ≈ 0.2 – 0.235 eV to produce the apparent agreement with the 1.945 eV ZPL.¹⁷ In small clusters like C₄₂H₄₂N[−], use of CI removes a significant correlation error of ≈ 0.6 eV in the DFT ΔE_V (³E). With only relaxation to be included, we are on somewhat firmer ground speculating on the ¹A₁, ³E ordering in C₄₂H₄₂N[−] than in bulk. Column 7 of Table 1 shows CI ΔE_V (³E_x) = 1.932 eV and ΔE_V (³E_y) = 1.958 eV lying slightly below ΔE_V (¹A₁) = 2.060 eV with relaxation neglected. In bulk, ³E relaxation is large; if larger than for ¹A₁

in C₄₂H₄₂N[−] we still have ³E < ¹A₁ on relaxation. Our stable C₄₂H₄₂N[−] cluster also shows NV centers could be designed from the bottom up: as ³E shifts upward with cluster size, we speculate such small clusters have ³E < ¹A₁ and quite different spin-polarization dynamics than larger clusters where the ordering changes to ³E > ¹A₁.

In conclusion we have determined the energies and order of the NV singlets using configuration interaction calculations. Because we find ¹E < ¹A₁, straightforward application of symmetry arguments to the intersystem crossings now predicts **S_x** and **S_y** polarization, contrary to the experimentally measured **S_z**. We deduce that some other, previously unknown, mechanism is working in the center to produce the key properties of qubit initialization and readout. Presently, the most likely candidate is coupling to nonsymmetric phonons,¹¹ followed by strain or electron–phonon terms beyond the Born–Oppenheimer approximation. Furthermore, the NV center in small nanodiamond clusters is chemically stable, motivating a bottom-up qubit approach, while optical properties will change significantly if the ³E level drops below ¹A₁ as the cluster size is reduced.

Acknowledgment. We thank SFI, HEA, and ICHEC for support.

REFERENCES AND NOTES

- (1) Brouri, R.; Beveratos, A.; Poizat, J.-P.; Grangier, P. *Opt. Lett.* **2000**, *25*, 1294–1296.
- (2) Kurtsiefer, C.; Mayer, S.; Zarda, P.; Weinfurter, H. *Phys. Rev. Lett.* **2000**, *85*, 290–293.
- (3) Jelezko, F.; et al. *Phys. Rev. Lett.* **2004**, *93*, 130501.
- (4) Loubser, J. H. H.; van Wyk, J. A. *Diamond Res.* **1977**, *1*, 11.
- (5) Jelezko, F.; Gaebel, T.; Popa, I.; Gruber, A.; Wrachtrup, J. *Phys. Rev. Lett.* **2004**, *92*, 76401.
- (6) Manson, N. B.; Harrison, J. P.; Sellars, M. J. *Phys. Rev. B* **2006**, *74*, 104303.
- (7) Rogers, L. J.; Armstrong, S.; Sellars, M. J.; Manson, N. B. *New J. Phys.* **2008**, *10*, 103024.
- (8) Goss, J. P.; Jones, R.; Breuer, S. J.; Briddon, P. R.; Öberg, S. *Phys. Rev. Lett.* **1996**, *77*, 3041–3044.
- (9) Gali, A.; Fyta, M.; Kaxiras, E. *Phys. Rev. B* **2008**, *77*, 155206.
- (10) van Oort, E.; Manson, N. B.; Glasbeek, M. J. *Phys. C* **1988**, *21*, 4385–4391.
- (11) Davies, G.; Hamer, M. F. *Proc. R. Soc. London, Ser. A* **1976**, *348*, 285–298.
- (12) Hossain, F. M.; Doherty, M. W.; Wilson, H. F.; Hollenberg, L. C. L. *Phys. Rev. Lett.* **2008**, *101*, 226403.
- (13) Larsson, J. A.; Delaney, P. *Phys. Rev. B* **2008**, *77*, 165201.
- (14) Lenef, A.; Rand, S. C. *Phys. Rev. B* **1996**, *53*, 13441–13445.
- (15) Coulson, C. A.; Kearsley, M. J. *Proc. R. Soc. London, Ser. A* **1957**, *241*, 433–454.
- (16) Gunnarsson, O.; Lundqvist, B. I. *Phys. Rev. B* **1976**, *13*, 4274–4298.

- (17) Gali, A.; Kaxiras, E. *Phys. Rev. Lett.* **2009**, *102*, 149703.
- (18) von Barth, U. *Phys. Rev. A* **1979**, *20*, 1693–1703.
- (19) Ahlrichs, R.; Bär, M.; Häser, M.; Horn, H.; Kölmel, C. *Chem. Phys. Lett.* **1989**, *162*, 165–169.
- (20) Delaney, P.; Larsson, J. A. *Phys. Procedia* **2009**, in press.
- (21) Greer, J. C. *J. Comput. Phys.* **1988**, *146*, 181.
- (22) Györfy, W.; Bartlett, R. J.; Greer, J. C. *J. Chem. Phys.* **2008**, *129*, 064103.
- (23) Zyubin, A. S.; Mebel, A. M.; Hayashi, M.; Chang, H. C.; Lin, S. H. *J. Comput. Chem.* **2008**, *30*, 119.
- (24) Dräbenstedt, A.; Fleury, L.; Tietz, C.; Jelezko, F.; Kilin, S.; Nizovtzev, A.; Wrachtrup, J. *Phys. Rev. B* **1999**, *60*, 11503.